The Lindvikskollen pegmatite at Kragerø: New mapping and mineral chemistry results

Erika De La Cruz [1], Axel Müller[1,2] and Muriel Erambert[3]

[1]Natural History Museum, P.O. 1172 Blindern, N-0318 Oslo, Norway (erikahd@uio.no)
[2]Natural History Museum, Cromwell Road, London SW7 5BD, UK (a.b.muller@nhm.uio.no)
[3]University of Oslo, Department of Geosciences, P.O. Box 1047 Blindern, N-0316 Oslo, Norway

Introduction

The Lindvikskollen pegmatite, 2.5 km west of Kragerø downtown, is part of the Kragerø pegmatite field and belongs to the older pegmatite group (1090-1030 Ma) of the Sveconorwegian orogeny (Rosing-Schow *et al.*, 2021). It is one of the oldest pegmatite mines in the south Norway where mining of K-feldspar started around 1890 (Friis, 1891). The pegmatite is the type locality of hellandite-(Y) (Brøgger 1903, 1906) and contains abundant black tourmaline with crystal sizes of up to 20 cm. Based on the accessory mineralogy comprising 'allanite', euxenite-(Y), fergusonite-(Y), 'aeschynite', and monazite-(Ce), the pegmatite is classified as niobium-yttrium-fluorine (NYF) type according to the family classification by Černý (1991). The tourmaline enrichment, however, is not common for NYF pegmatites and the source of B of the Lindvikskollen and other Kragerø pegmatites is still debated. This contribution is part of ongoing investigations of the Kragerø pegmatites lead by the Norwegian Center for Mineralogy of the Natural History Museum of Oslo aiming to better understand the formation of the these pegmatites and their mineral paragenesis.

Mineralogy and zoning of the Lindvikskollen pegmatite

The Lindvikskollen pegmatite forms an irregular body, which is about 500 m long in E-W direction and up to 200 m wide. Figure 1 shows the complex surface outline of the pegmatite body mapped recently by De La Cruz (2021). The pegmatite intruded a massive metagabbro, which forms the Storkollen-Lindvikskollen hill. The metagabbro was albitized to albitite at the W/NW contact of the pegmatite prior to pegmatite melt emplacement. The major minerals are K-feldspar, plagioclase (oligoclase), albite, quartz and biotite. The predominant accessory mineral is black tourmaline. Additional accessory minerals beside the named ones are titanite, muscovite, ilmenite, rutile, magnetite, 'gadolinite', fluorapatite, phenakite, bastnäsite-(Ce), caysichite-(Y), chernovite-(Y), hingganite-(Y), kainosite-(Y), thorite, zircon, and xenotime-(Y).

The pegmatite exhibits principally three mineralogical zones: megacrystic, relative equi-granular pegmatitic granite considered in the following as wall zone. The wall zone contains multiple cores (three cores were identified during fieldwork in 2020) formed predominantly of massive quartz, which are several meters in size (Fig. 1). Up to 20 cm large tourmalines occur sparsely in the quartz cores. The cores are surrounded by intermediate zones (also called blocky zones) consisting predominantly of euhedral to sub-euhedral K-feldspar megacrysts of 0.2 to 2 m in size. In addition, the intermediate zones contain quartz, muscovite and tourmaline. Occasionally up to 2 m large biotite sheets are found in the intermediate zone or in the wall zone close to the intermediate zone. In the intermediate zone

surrounding the core in the East mine, up to 30 cm large crystals of allanite-(Ce) and fergusonite-(Y) were observed.

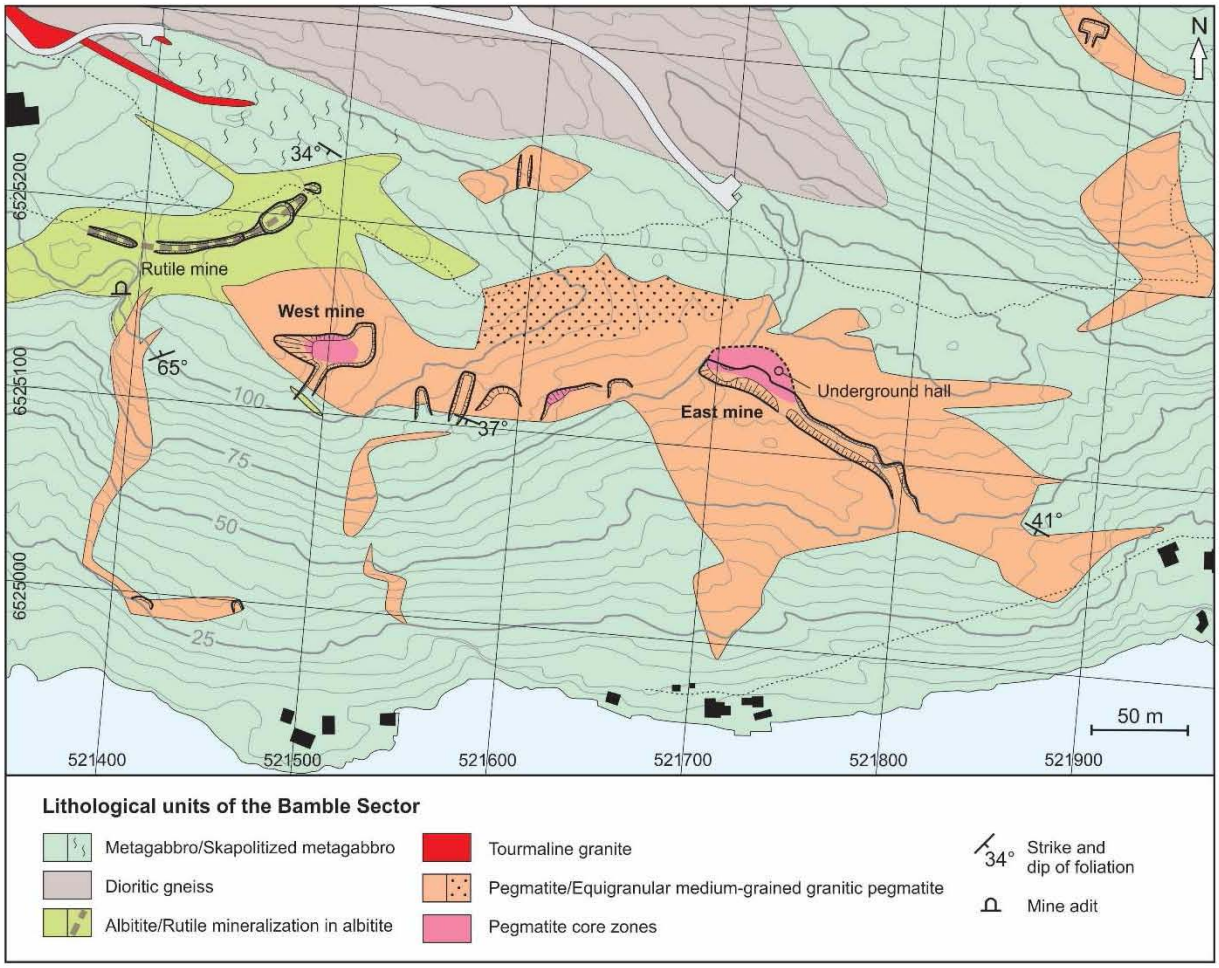

***Figure 1**. Geological map of the Lindvikskollen area, west of Kragerø. Modified from De La Cruz (2021).*

Chemistry of mica, feldspar and tourmaline

Electron probe micro analyses (EPMA) were performed on five *mica* samples originating from different zones of the Lindvikskollen pegmatite. Dark micas from the wall and intermediate zones have relative consistent compositions and are classified as magnesian siderophyllite (Fig. 2). The only exception is the slightly higher Al content of the mica from the East mine compared to the micas from the West mine (Table 1). White mica (sample 12062019), collected from the intermediate zone close to the quartz core of the West mine (Fig. 1) has lithian muscovite composition. The Li content of mica was calculated according to Tischendorf *et al.* (2001), which might lead to an slight overestimation of the Li content in white mica (Rosing-Schow *et al.*, 2018). The chemistry of dark micas fall in the range of other Sveconorwegian pegmatites from southern Norway. The white muscovite has, however, a rather unique, chemically highly evolved composition.

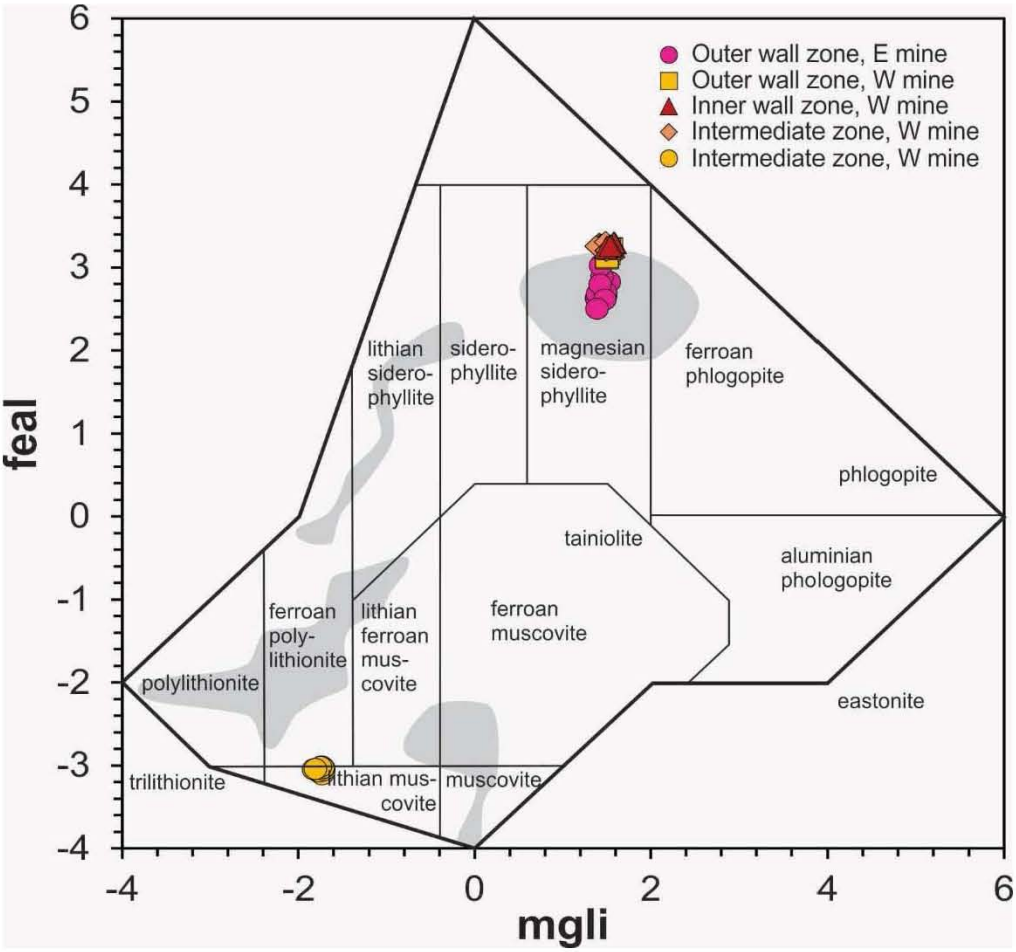

Figure 2. *Classification diagram of mica after Tischendorf et al. (2001) illustrating compositions of dark and white micas of the Lindvikskollen pegmatite. The grey fields represent mica compositions of other Sveconorwegian pegmatites in southern Norway according to Rosing-Schow et al. (2018). mgli = Mg – Li (atoms per formular unit); feal = Fe^{tot} + Mn + Ti - Al^{VI} (atoms per formular unit).*

The average composition of *K-feldspar* from Lindvikskollen is $Or_{95}Ab_5An_0$ (n = 70) and of *plagioclase* $Or_1Ab_{88\text{-}92}An_{7\text{-}11}$ (n = 20). K-feldspar samples, collected along traverses across the pegmatite body, have relative consistent and overlapping compositions (Table 2, Fig. 3A). K-feldspars of the East mine, however, have slightly lower Sr indicating a higher fractionation degree of the melt in the eastern part of the pegmatite body. Compared to compositions of K-feldspars from other pegmatite localities worldwide, the Lindvikskollen K-feldspars have the most primitive composition (Fig. 3B). The Lindvikskollen plagioclases show distinct chemical variations related to the pegmatite zoning: Plagioclase from the wall zone has oligoclase composition $Or_1Ab_{88}An_{11}$ (n = 10) while those from the intermediate zone have more evolved Ca-rich albite composition $Or_1Ab_{92}An_7$ (n = 10). It is noteworthy that plagioclase does not occur in the pegmatite cores.

Table 1. *Average compositions of micas from the Lindvikskollen pegmatite measured with EPMA. The low totals of major elements are due to the non-measured H_2O content of micas. n = number of analyses, σ = standard deviation.*

	Magnesian siderophyllite 06071911 East mine Outer wall zone		Magnesian siderophyllite 12062011 West mine Outer wall zone		Magnesian siderophyllite 12062005 West mine Inner wall zone		Magnesian siderophyllite 12062002 West mine Intermediate zone		Lithian muscovite 12062019 West mine Intermediate zone	
n	10	σ	10	σ	10	σ	10	σ	10	σ
Major elements (wt.%)										
SiO_2	36.14	0.37	35.81	0.15	36.23	0.17	36.27	0.24	45.25	0.32
TiO_2	2.68	0.17	3.62	0.05	3.63	0.04	3.87	0.04	0.12	0.02
Al_2O_3	15.75	0.30	13.95	0.09	13.70	0.10	13.84	0.14	35.17	0.27
FeO	21.70	0.67	21.40	0.18	21.73	0.16	21.90	0.21	1.94	0.10
MnO	0.02	0.02	0.55	0.05	0.65	0.03	0.36	0.03	0.01	0.01
MgO	8.48	0.30	8.45	0.10	9.01	0.09	8.63	0.16	0.18	0.05
CaO	0.00	0.00	0.00	0.00	0.00	0.00	0.01	0.02	0.00	0.01
Li_2O_{calc}	0.79	0.11	0.69	0.04	0.81	0.05	0.82	0.07	3.42	0.09
Na_2O	0.05	0.01	0.03	0.01	0.04	0.01	0.04	0.01	0.21	0.02
K_2O	9.64	0.20	9.57	0.06	9.75	0.07	9.82	0.10	11.23	0.12
Rb_2O	0.14	0.02	0.07	0.02	0.09	0.03	0.07	0.02	0.04	0.03
F	0.43	0.07	0.58	0.04	0.79	0.10	0.78	0.11	0.05	0.03
O=F	0.18	0.03	0.24	0.02	0.33	0.04	0.33	0.05	0.02	0.01
Total	95.63	0.46	94.48	0.34	96.11	0.30	96.06	0.50	97.60	0.48
Atoms per formula unit										
Si	5.517	0.015	5.546	0.018	5.508	0.019	5.512	0.012	5.885	0.018
Al (IV)	2.483	0.015	2.454	0.018	2.455	0.018	2.468	0.028	2.115	0.018
Z	8.000	0.000	8.000	0.000	7.963	0.018	7.980	0.025	8.000	0.000
Al (VI)	0.350	0.040	0.091	0.019	0.000	0.000	0.012	0.022	3.275	0.022
Fe(II)	2.771	0.107	2.771	0.024	2.763	0.021	2.783	0.025	0.211	0.011
Li	0.482	0.061	0.430	0.025	0.497	0.029	0.502	0.040	1.787	0.040
Mn	0.003	0.003	0.073	0.006	0.084	0.004	0.046	0.004	0.001	0.002
Ti	0.308	0.022	0.422	0.005	0.415	0.004	0.442	0.005	0.012	0.002
Mg	1.928	0.057	1.952	0.017	2.042	0.021	1.955	0.029	0.035	0.010
Y	5.842	0.032	5.738	0.025	5.801	0.033	5.741	0.033	5.321	0.027
K	1.876	0.030	1.890	0.015	1.891	0.020	1.904	0.020	1.863	0.023
Na	0.014	0.004	0.010	0.003	0.013	0.004	0.012	0.003	0.052	0.006
Ca	0.000	0.000	0.000	0.000	0.000	0.000	0.001	0.003	0.000	0.001
Rb	0.014	0.002	0.007	0.002	0.008	0.003	0.006	0.002	0.003	0.002
X	1.904	0.030	1.907	0.014	1.912	0.020	1.923	0.019	1.919	0.021
OH	3.794	0.034	3.717	0.019	3.623	0.047	3.626	0.052	3.979	0.014
F	0.206	0.034	0.283	0.019	0.377	0.047	0.374	0.052	0.021	0.014
Total	19.746	0.037	19.645	0.021	19.676	0.036	19.644	0.028	19.240	0.016
mgli	1.446	0.049	1.522	0.019	1.545	0.037	1.453	0.040	-1.752	0.040
feal	2.732	0.151	3.175	0.047	3.262	0.024	3.259	0.036	-3.051	0.030
Fe nr.	0.590	0.015	0.587	0.003	0.575	0.002	0.587	0.005	0.860	0.034

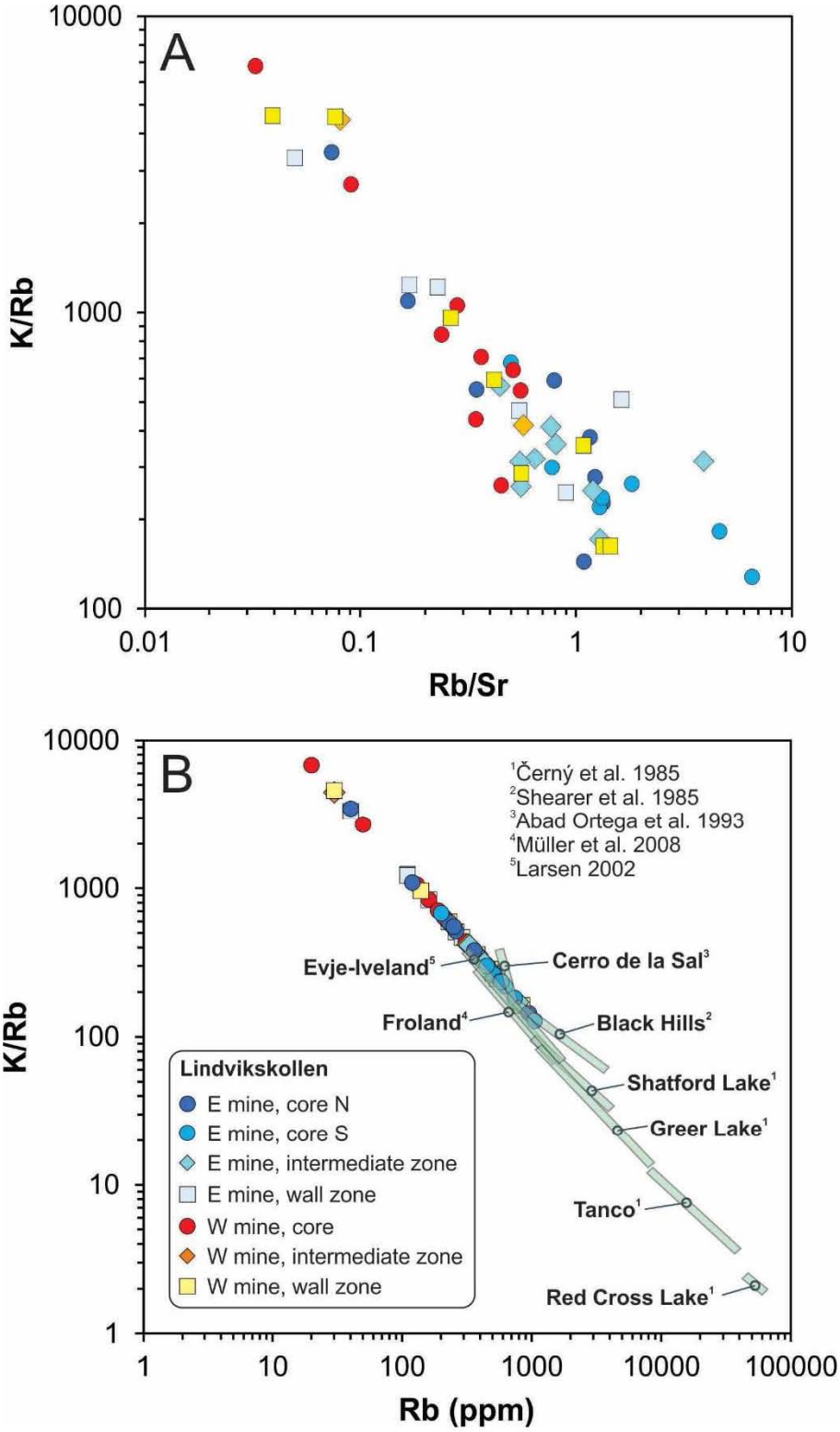

***Figure 3**. **A**: Rb/Sr versus K/Rb of K-feldspar illustrating the chemical variability within the Lindvikskollen pegmatite. **B**: Rubidium versus K/Rb of K-feldspar from the Lindvikskollen pegmatite compared with K-feldspar composition from other pegmatite provinces around the world. Modified from Larsen (2002). Element concentrations were measured by EPMA.*

.

	Plagioclase 06071910 East mine Wall zone		Plagioclase 06071907 East mine Intermediate zone		K-feldspar 06071902 East mine Core zone		K-feldspar 06071904 East mine Core zone		K-feldspar 06071906 East mine Intermediate zone		K-feldspar 06071909 East mine Wall zone		K-feldspar 12062010 West mine wall zone		K-feldspar 12062006 West mine Intermediate zone		K-feldspar 12062001 West mine Core zone	
n	10	σ	10	σ	10	σ	10	σ	10	σ	10	σ	10	σ	10	σ	10	σ
SiO_2	66.20	0.16	67.08	0.30	64.98	0.33	64.87	0.26	64.83	0.12	65.09	0.19	64.72	0.26	64.72	0.11	64.52	0.39
Al_2O_3	21.00	0.17	20.20	0.13	17.94	0.20	17.92	0.11	17.84	0.10	17.93	0.07	17.77	0.12	17.92	0.13	17.86	0.18
FeO	0.06	0.03	0.05	0.02	0.04	0.02	0.04	0.03	0.02	0.02	0.03	0.02	0.03	0.02	0.05	0.02	0.04	0.02
CaO	2.35	0.05	1.60	0.12	0.02	0.03	0.00	0.00	0.00	0.00	0.00	0.00	0.00	0.00	0.00	0.00	0.00	0.00
Na_2O	10.57	0.07	10.94	0.12	0.48	0.07	0.59	0.09	0.52	0.04	0.68	0.14	0.51	0.07	0.70	0.11	0.52	0.10
K_2O	0.11	0.03	0.12	0.03	16.42	0.26	16.25	0.10	16.34	0.08	16.14	0.15	16.44	0.12	16.05	0.18	16.29	0.15
BaO	<0.01	-	<0.01	-	<0.01	-	<0.01	-	<0.01	-	0.01	0.02	<0.01	-	0.08	0.03	0.05	0.04
SrO	0.05	0.02	0.04	0.02	0.05	0.03	0.04	0.03	0.06	0.03	0.04	0.03	0.06	0.02	0.06	0.01	0.08	0.03
Rb_2O	<0.01	-	<0.01	-	0.04	0.03	0.05	0.04	0.04	0.02	0.02	0.02	0.03	0.04	<0.01	-	0.02	0.02
Total	100.34	0.25	100.02	0.38	99.97	0.25	99.76	0.34	99.66	0.15	99.95	0.13	99.58	0.26	99.58	0.20	99.37	0.51
An	10.9	0.2	7.4	0.6	0.1	0.2	0.0	0.0	0.0	0.0	0.0	0.0	0.0	0.0	0.0	0.0	0.0	0.0
Ab	88.5	0.2	91.9	0.6	4.2	0.7	5.2	0.8	4.7	0.3	6.0	1.2	4.5	0.6	6.2	1.0	4.6	0.9
Or	0.6	0.1	0.6	0.2	95.7	0.8	94.8	0.8	95.3	0.3	94.0	1.2	95.5	0.6	93.8	1.0	95.4	0.9

Table 2. *Average compositions of plagioclase and K-feldspar from the Lindvikskollen pegmatite measured with EPMA (wt.%). n = number of analyses, σ = standard deviation.*

The major and minor element compositions of *tourmalines* were determined by EPMA. Average concentrations are given in Table 3. The contents of Li_2O, B_2O_3, and H_2O were calculated using an Excel calculation spreadsheet. In this approach, B_2O_3 and H_2O were obtained assuming fixed B at 3 atoms per formula unit (apfu) and OH + F at 4 apfu. Lithium was calculated using the method of Burns *et al.* (1994). The Lindvikskollen tourmalines belong to the alkali-tourmaline group based on the dominant occupancy of the *X*-site and classify as schorl, with Mg/(Mg+Fe) values between 0.22 and 0.49 (Fig. 4). The tourmalines from the wall, intermediate and cores zones of the Lindvikskollen pegmatite have consistent Mg- and Fe-rich compositions. This finding contrasts studies from other tourmaline-bearing pegmatites worldwide, which show commonly a great variation of tourmaline chemistries with in pegmatite bodies (*e.g.* Simmons *et al.* 2005; Falster *et al.* 2018).

Table 3. *Average compositions of tourmaline of the Lindvikskollen pegmatite measured with EPMA. From De La Cruz (2021). n = number of analyses, σ = standard deviation.*

	Schorl Wall zone		Schorl Intermediate zone		Schorl Core zone	
n	26	σ	97	σ	74	σ
Major elements (wt.%)						
SiO_2	34.97	0.37	35.21	0.30	35.17	0.29
Al_2O_3	25.06	0.61	25.31	1.16	24.19	0.59
TiO_2	1.22	0.21	1.19	0.36	1.31	0.14
FeO	17.27	1.22	16.24	1.23	16.28	0.87
MgO	4.75	0.99	5.36	0.79	5.91	0.72
MnO	0.16	0.03	0.18	0.06	0.19	0.04
Na_2O	2.21	0.18	2.15	0.11	1.98	0.12
$B_2O_{3\ calc}$	10.04	-	10.11	-	10.06	-
CaO	1.01	0.36	1.15	0.24	1.49	0.26
Li_2O_{calc}	0.23	-	0.24	-	0.29	-
H_2O_{calc}	3.38	-	3.36	-	3.36	-
K_2O	0.10	0.02	0.08	0.01	0.08	0.01
F	0.18	0.10	0.27	0.10	0.24	0.09
Total	100.49	-	100.75	-	100.43	-
Formula proportions in atoms per formula unit						
Si	6.06	-	6.05	-	6.08	-
Al	5.11	-	5.13	-	4.92	-
Ti	0.16	-	0.15	-	0.17	-
Fe^{2+}	2.50	-	2.34	-	2.35	-
Mg	1.22	-	1.37	-	1.52	-
Mn	0.02	-	0.03	-	0.03	-
Na	0.74	-	0.71	-	0.66	-
B	3.00	-	3.00	-	3.00	-
Ca	0.19	-	0.21	-	0.28	-
Li	0.16	-	0.17	-	0.20	-
OH	3.90	-	3.85	-	3.87	-
K	0.02	-	0.02	-	0.02	-
F	0.10	-	0.15	-	0.13	-
X Al	-0.62	-	-0.62	-	-0.77	-
X vac	0.05	-	0.06	-	0.04	-

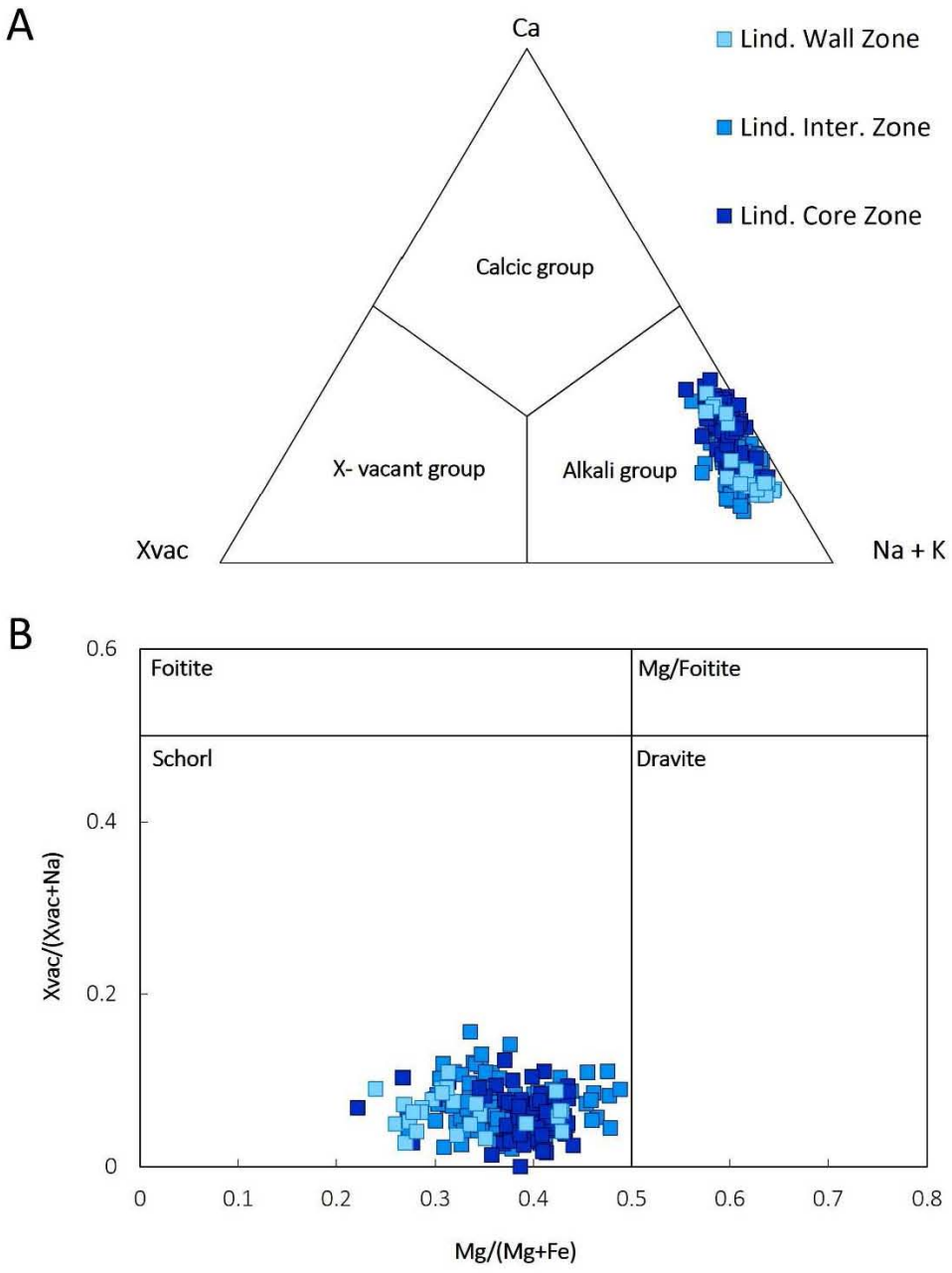

Figure 4. ***A****: Chemistry of Lindvikskollen tourmalines from the different pegmatite zones plotted in the classification diagram by Henry et al. (2011) using the occupancy of the X-site.* ***B****: Mg/(Mg+Fe) vs Xvac/(Xvac+Na) classification diagram according to Henry et al. (2011). All Lindvikskollen tourmalines plot in the schorl field. Xvac = X-site vacancy.*

Summary

New mapping of the Lindvikskollen pegmatite revealed a complex shape and zoning of the intrusive body. The pegmatite exhibits three mineralogical zones: wall, intermediate and core zones. The pegmatite has multiple quartz cores surrounded by megacrystic intermediate zones and coarse- to very

coarse-grained wall zones. The chemistry of dark mica and feldspar documents a very primitive granitic composition of the Lindvikskollen pegmatite. In fact, the pegmatite represents one of the most primitive granitic pegmatites worldwide. The primitive chemistry seems to be in contrast of the elevated B content of the melt documented by the common occurrence of black tourmaline across the entire pegmatite body. Boron enrichments are typical for fractionated granite melts and lithium-cesium-tantalum (LCT) enriched pegmatites. It is suggested that the melt source rock must have been relative rich in B. The relative consistent chemistry of K-feldspar, plagioclase and tourmaline record relative limited pegmatite-internal melt fractionation. Common tourmaline in the wall, intermediate and core zone document that there was sufficient Fe in the melt to crystallize schorl until the final stage of pegmatite crystallization.

References

Abad Ortega, M.D.M., Hach-Alí, P.F., Martin-Ramos, J.D. & Ortega-Huertas, M. (1993): The feldspars of the Sierra Albarrana granitic pegmatites, Cordoba, Spain. *The Canadian Mineralogist* **31**, 185-202.

Brøgger, W.C. (1903): Über Hellandit, ein neues Mineral (Vorläufige Mittheilungen). *Nyt Magazin for Naturvidenskaberne* **41**, 213-221.

Brøgger, W.C. (1906): Hellandit von Lindvikskollen bei Kragerö, Norwegen. *Zeitschrift für Kristallographie und Mineralogie* **42**, 417-439.

Burns, P.C., Macdonald, D.J. & Hawthorne, F.C. (1994): The crystal chemistry of manganese-bearing elbaite. *The Canadian Mineralogist* **32**, 31-41.

Černý, P. (1991): Rare-element granitic pegmatites. Part 1: Anatomy and internal evolution of pegmatite deposits. Part 2: Regional to global environments and petrogenesis. *Geoscience Canada* **18**, 49–81.

Černý, P., Meintzer, R.E. & Anderson, A.J. (1985): Extreme fractionation in rare-element granitic pegmatites: selected examples of data and mechanisms. *The Canadian Mineralogist* **23**, 381-421.

De La Cruz, E. (2021): *Tourmaline of the Kragerø pegmatites: The source of boron and its implication for the melt formation of Sveconorwegian pegmatites.* MSc thesis, University of Oslo.

Falster, A.U., Simmons, W.B., Webber, K.L. & Boudreaux, A.P. (2018): Mineralogy and geochemistry of the Erongo sub-volcanic granite-miarolitic-pegmatite complex, Erongo, Namibia. *The Canadian Mineralogist* **56**, 425-449.

Friis, J.P. (1891): Feldspat, kvarts og glimmer, deres forekomster og anvendelse i industrien. *Norges Geologiske Undersøkelse* **1**, 50-69.

Henry, D.J., Novák, M., Hawthorne, F.C., Ertl, A., Dutrow, B.L., Uher, P. & Pezzotta, F. (2011): Nomenclature of the tourmaline-supergroup minerals. *American Mineralogist* **96**, 895-913.

Larsen, R.B. (2002): The distribution of rare-earth elements in K-feldspar as an indicator of petrogenetic processes in granitic pegmatites: Examples from two pegmatite fields in southern Norway. *The Canadian Mineralogist* **40**, 137-151.

Müller, A., Ihlen, P.M. & Kronz, A. (2008): Quartz chemistry in polygeneration Sveconorwegian pegmatites, Froland, Norway. *European Journal of Mineralogy* **20**, 447-463.

Rosing-Schow N., Müller A. & Friis H. (2018): A comparison of the mica chemistry of the pegmatite fields in southern Norway. *The Canadian Mineralogist* **56**, 463-488.

Shearer, C.K., Papike, J.J. & Laul, J.C. (1985): Chemistry of potassium feldspar from three zoned pegmatites, Black Hills, South Dakota: implications concerning pegmatite evolution. *Geochimica at Cosmochimica Acta* **49**, 663-673.

Simmons, W.B., Laurs, B.M., Falster, A.U., Koivula, J.I. & Webber, K.L. (2005): Mt. Mica: A renaissance in Maine's gem tourmaline production. *Gems & Gemology* **41**, 150–163.

Tischendorf, G., Förster, H.-J. & Gottesmann, B. (2001): Minor- and trace-element composition of trioctahedral micas: a review. *Mineralogical Magazine* **65**, 249–276.

Rosing-Schow, N., Romer, R.L., Müller, A., Corfu, F., Škoda, R. & Friis, H. (2021): Breaking the paradigm: Orogen-wide, two-stage pegmatite formation by anatexis during the assembly of Rodinia. *Precambrian Research* (in review).

Soares, D., Beurlen, H., De Brito Barreto, S. & Reis Rodrigues Da Silva, M. (2008): Compositional variation of tourmaline-group minerals in the Borborema Pegmatite Province, northeastern Brazil. *The Canadian Mineralogist* **46**, 1097-1116.